

## Stage Transformation and Staging Disorder in Graphite Intercalation Compounds

M. E. Misenheimer<sup>(a)</sup> and H. Zabel

*Department of Physics and Materials Research Laboratory, University of Illinois, Urbana, Illinois 61801*  
(Received 15 March 1985)

Stage purity and staging transitions of potassium-graphite intercalation compounds have been investigated *in situ* by high-resolution x-ray scattering. The positions and profiles of (00L) Bragg reflections indicate staging disorder in thermal equilibrium for all compounds larger than stage 2, which increases with increasing stage number. The transition region between stages exhibits a miscibility gap for stage mixing whose size decreases with higher stages. The results are compared with recent theories on the staging of graphite intercalation compounds.

PACS numbers: 64.70.Kb, 61.10.Fr, 61.70.Ph

Graphite intercalation compounds represent a unique model system for the study of the ground state of a one-dimensional (1D) system. They consist of a periodic sequence of graphite basal planes and intercalate layers stacked along the layer normal, usually referred to as staging.<sup>1</sup> It has recently been pointed out by Bak and Jensen<sup>2</sup> that the staging phenomenon is homologous to a 1D Ising model with long-range anti-ferromagnetic interactions in an external magnetic field.<sup>3</sup> This model predicts a complete devil's staircase of commensurate stage numbers. Safran<sup>3</sup> calculated the first staging phase diagram based on an Ising-type Hamiltonian with attractive intercalant-intercalant interaction within the same plane and repulsive interaction between separated planes. The latter was assumed to be electrostatic in nature and of the form  $V = V_0/|Z|^\alpha$ , where  $V_0$  depends on the total charge transfer between intercalant and graphite layer, and  $|Z|$  is the distance between two intercalate layers. Together with an entropy term for the in-plane alkali-metal mixing, this model predicts stability regions for pure stages and transitions of first order between ordered stages.

The range of the interaction,  $\alpha$ , is related to the distribution of charge over the intervening graphite planes. Values from 1 to 4 have been used for calculation of the phase diagram.<sup>4</sup> As the stage number is increased, the distance between intercalate layers approaches the range of the interaction and the difference in energy between a pure- and disordered-stage graphite intercalation compound becomes negligible. By a disordered stage we mean a mixture of different stage packages, where a stage- $n$  package consists of an intercalate layer and  $n$  graphite layers. Kirczenow<sup>5</sup> recently showed that adding an entropy term for complete stage packages in a Hamiltonian based on the intercalate electrostatic interaction would allow for stage disorder in high-stage compounds. His model also shows that the disorder is strongly related to the intercalate in-plane domain size. For finite domain sizes the stage transition becomes continuous with a smoothly varying fraction of the dominant stage

number  $n$  across the transition region. A continuous stage transition has also been predicted by Forgacs and Uimin.<sup>6</sup>

In this Letter we report the first x-ray study of stage disorder of alkali-metal-graphite intercalation compounds in thermal equilibrium. Stage disorder has been observed previously in acceptor<sup>7</sup> and donor compounds.<sup>8,9</sup> However, these measurements were carried out *ex situ* and therefore were not decisive towards whether the observed one-dimensional disordered structure would remain in thermodynamic equilibrium and if the amount of stage- $(n \pm 1)$  admixture in a nominal stage- $n$  compound is fixed or a continuous function of the thermodynamic variables. In the present *in situ* x-ray experiment we obtained for the first time evidence that all stages  $n \geq 2$  exhibit, in thermal equilibrium, stage mixing, and that the percentage of stage- $(n+1)$  packages in a stage- $n$  compound continuously increases when approaching the  $n \rightarrow n+1$  transition. Although the stage mixing increases with increasing stage number, there remains a finite miscibility gap of stage mixing at the staging transition.

The present experiments were performed with Mo  $K\alpha$  radiation in reflection geometry on a triple-axis spectrometer, with use of (111) Si crystals in  $+1, -1$  configuration. Triple-axis scattering geometry was essential in this study in order to distinguish between reflection broadenings which are due to stage disorder and those due to sample transparency.<sup>10</sup> Pristine highly oriented pyrolytic graphite of grade ZYB from Union Carbide and potassium metal with a state purity of 99.8% from A. D. MacDay were used.

Figure 1(a) is a plot of diffracted intensity versus scattering vector  $Q = (4\pi/\lambda)\sin(\theta)$ , for the stage-5 (005) reflection at a sample temperature of 455 °C and a potassium temperature of 230 °C. The stage number was determined from the complete (00L) profile by use of the relation  $L_{\max} = n + 1$ , where  $L_{\max}$  is the index of the reflection with highest intensity. As the sample temperature was lowered, at constant alkali-metal temperature, this reflection was seen to shift

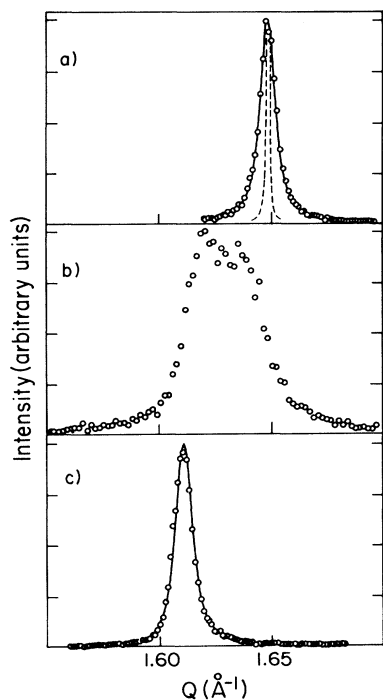


FIG. 1. Intensity as a function of scattering vector,  $Q$ , for  $(00L)$  reflections taken *in situ* at constant chemical potential. (a) Stage-5 (005) at  $T_G = 455^\circ\text{C}$ . The solid line is a fit using Hendricks-Teller (HT) theory, convoluted with instrumental resolution; the dashed line shows the instrumental resolution. (b) Superposition of two reflections in the transition region to stage 4.  $T_G = 450^\circ\text{C}$ . With time the lower- $Q$  reflection grows at the expense of the higher. (c) Stage-4 (004) at  $T_G = 444^\circ\text{C}$ . The solid line is again a fit using HT theory. Notice the shift and broadening of the two reflections in (b) compared to (a) and (c).

continuously toward lower  $Q$  values and to broaden. This shift is contrary to what would be expected solely from the thermal expansion of the sample. At each temperature the sample was given time to equilibrate and several measurements of the same profile were taken to ensure that equilibrium had been reached. As the successive lowering of the sample temperature was continued, the stage-4 (004) reflection appeared at  $450^\circ\text{C}$ , Fig. 1(b). At this temperature the stage-4 reflection grew as a function of time and at the expense of the stage-5 reflection. In the transition region a dramatic increase in the peak widths of both reflections was noticed. After equilibrium had been achieved the sample temperature was again successively lowered. The (004) reflection was seen to continuously shift to lower  $Q$  towards its "ideal" stage-4 position and to become narrower. Figure 1(c) shows the reflection at a sample temperature of  $444^\circ\text{C}$ . Similar observations were made at the stage  $4 \rightarrow 3$  transition. The stage  $2 \rightarrow 1$  transition exhibited the same

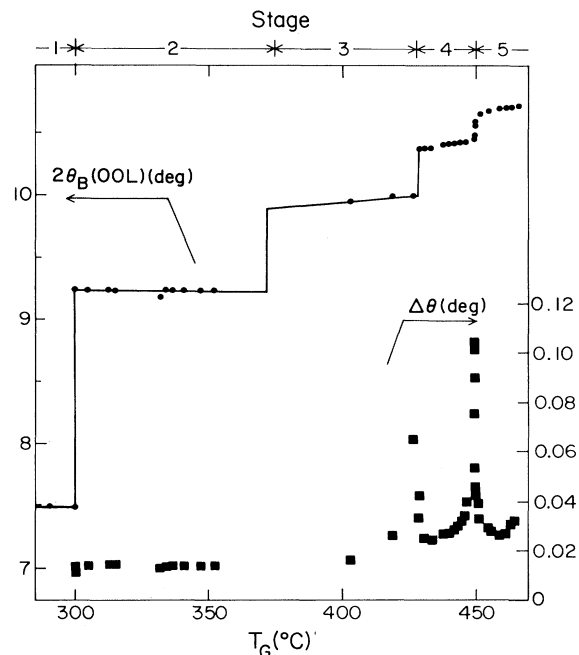


FIG. 2.  $2\theta$  positions and half widths at half maximum intensity as obtained from Lorentzian fits to the  $(00L)$  Bragg profiles during *in situ* staging transformations at constant alkali-metal temperature,  $T_K = 230^\circ\text{C}$ .

behavior as in our previous measurements with less resolution<sup>11</sup>: In contrast to the higher-stage transitions, there was no observable shifting of the reflections from their pure-stage positions nor broadening of the reflections either within a stage or during the transition.

Figure 2 summarizes the results of the constant alkali-metal temperature, i.e., constant chemical potential, experiment. The half width at half maximum intensity of the stage- $n$  ( $00n$ ) reflections and peak positions, both in degrees  $2\theta$ , are plotted as a function of the sample temperature. These parameters have been obtained from fits of the Bragg reflections with Lorentzian profiles. The continuous shift in position with temperature is clearly evident as is the increase in width near the transition regions, for high stages. The slight negative slope in the stage-1 and stage-2 results is consistent with thermal expansion.

Measurements were also taken at constant sample temperature and varying chemical potential. The same continuous changes in peak position and peak width were seen within a stage (Fig. 3). Stage transitions again exhibited a discontinuous change through a two-phase region evidenced by a superposition of two sets of reflection as in Fig. 1(b). Since the latter measurements have been taken at constant sample temperature, none of the peak shifts can be attributed to thermal expansion. Both the shift and the width of the

(00L) reflections clearly indicate that stage disorder exists in thermodynamic equilibrium and increases with higher stage numbers as well as close to staging transitions.

In order to extract the fraction  $f_m = \nu_m / \sum \nu_i$  of stage- $m$  packages in a nominal stage- $n$  compound, where  $\nu_m$  is the number of packages consisting of  $m$  host layers sandwiched between a pair of intercalate layers, we have analyzed the staging disorder using the Hendricks-Teller (HT) model<sup>12</sup> for the x-ray structure factor of one-dimensionally disordered lattices. In the HT theory the averaged diffracted intensity from a stack of  $r$  different and uncorrelated stage packages with frequency of occurrence  $f_n$  and stage form factor  $F_n$  is

$$\langle I \rangle = \sum_{n=1}^r f_n |F_n|^2 + 2 \sum_{m=1}^r \sum_{n=1}^r f_m f_n |F_m| |F_n| \frac{\cos(\phi_m + \phi_n + \alpha_m - \alpha_n) - K \cos(\phi_m + \phi_n - \bar{\phi} + \alpha_m - \alpha_n)}{1 - 2K \cos \bar{\phi} + K^2}, \quad (1)$$

where  $\phi_n$  is the phase difference due to the thickness of a package. The average phase factor  $\bar{\phi}$  and the constant  $K$  are implicitly defined by

$$\begin{aligned} \sum_{n=1}^r f_n \sin(2\phi_n - \bar{\phi}) &= 0, \\ \sum_{n=1}^r f_n \cos(2\phi_n - \bar{\phi}) &= K. \end{aligned} \quad (2)$$

The stage form factor  $F_n(\mathbf{Q})$  follows from the stage- $n$  structure factor

$$\tilde{F}_n(\mathbf{Q}) = f_A(\mathbf{Q}) = f_C(\mathbf{Q}) e^{i\phi_n} \frac{\sin(n\phi_0)}{\sin(\phi_0)} \quad (3)$$

via

$$F_n(\mathbf{Q}) = \tilde{F}_n(\mathbf{Q}) e^{-i\phi_n} = |F_n(\mathbf{Q})| e^{i\alpha_n}, \quad (4)$$

with

$$\phi_{0,n} = \frac{1}{2} \mathbf{Q} \cdot \mathbf{d}_{0,n}, \quad (5)$$

where  $\mathbf{d}_{0,n}$  are the pristine-graphite and stage- $n$  layer repeat distances, respectively.  $f_{A,C}(\mathbf{Q})$  are the atomic form factors of the alkali-metal and carbon atoms, including the layer stoichiometry of the compounds. The HT intensity was convoluted with the experimental resolution and then fitted to the observed reflection profile, with use of the package fractions  $f_m$  as fit parameters. An experimental resolution function, shown as a dashed line in Fig. 1(a), was obtained from the stage-2 (002) reflection, close to the stage-1 transition which does not exhibit any positional shifts or line broadenings characteristic for stage mixing (see Figs. 2 and 3). Typical fit results are shown as solid lines in Figs. 1(a) and 1(c). Note that the calculated profile and position of the Bragg reflection for the disordered stage determine the quality of the fit. Since both parameters are highly correlated a good fit is only obtained by a well defined set of package fractions  $f_n$ . The stage-5 reflection in Fig. 1(a) is represented by a mixture of 71% stage-5, 19% stage-4, and 10% stage-6 packages; the stage-4 reflection in Fig. 1(c) is represented by a mixture of 94% stage-4, 4% stage-5, and 2% stage-3 packages. The accuracy of the fit parameters is better than  $\pm 1\%$ . Bragg reflections in the transition region, like in Fig. 1(b), were not fitted by the HT intensity since these reflections are time dependent and do not represent an equilibrium state.

Figure 4 shows the fraction of the stage- $n$  packages,  $f_n$ , obtained from the HT analysis as a function of the chemical potential. According to this analysis, stage-1 compounds are always purely staged compounds throughout the stability region, containing only stage-1 packages. Stage-2 compounds reach pure-stage order near the stage-1 transition, but show some stage mixing with stage-1 and -3 packages close to the stage 2  $\rightarrow$  3 transition. Stage-3 compounds never become purely staged, the maximum stage-3 fraction being 98%. The minority stages present are 2 and 4 with increasing fractional amounts as either the stage 3  $\rightarrow$  2 or the stage 3  $\rightarrow$  4 transition is approached.

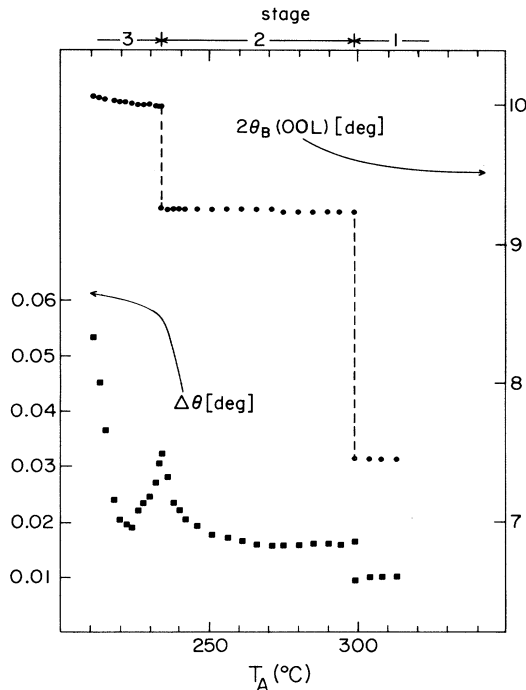


FIG. 3. Same as Fig. 2 but for measurements at constant sample temperature,  $T_G = 381^\circ\text{C}$ .

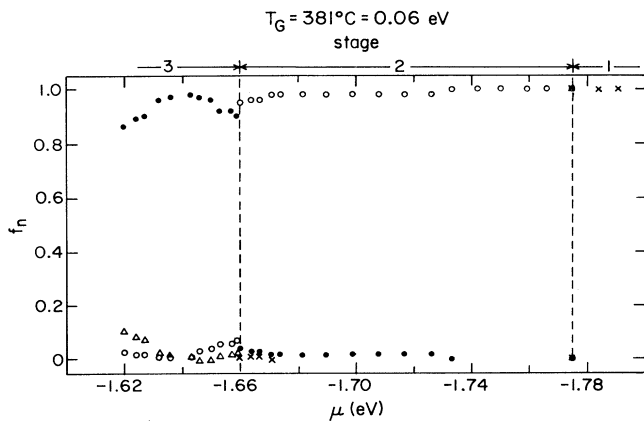


FIG. 4. Fraction  $f_n$  of stage- $n$  packages as a function of the chemical potential at constant sample temperature. Arrows on top of the figure indicate stability region of a stage- $n$  compound and dashed lines the staging transition. Fractional staging is indicated by the following: crosses, stage 1; open circles, stage 2; solid circles, stage 3; and triangles, stage 4.

Qualitatively, the present results are in excellent agreement with Kirczenow's staging model.<sup>5</sup> Stage mixing is seen to be a fundamental ingredient of the staging phase diagram. The composition of a mixed stage varies continuously across the stability region of the dominant stage and the maximum purity that a stage can reach decreases with increasing stage number. However, there are a few significant discrepancies with the staging model discussed above. For the large intercalate domain sizes of about 5000 Å in donor compounds,<sup>10</sup> stage mixing should have been rather negligible. In fact, the present results resemble more the predictions for acceptor compounds, which exhibit smaller domain sizes and less charge transfer between the intercalate and graphite layers.<sup>13</sup> Thus, it appears that the electrostatic repulsion in donor compounds has been overestimated and a power law with  $\alpha = 4$  may be more realistic. Also, all staging transitions measured show a discontinuous change in the fractional amount of the dominant stage packages, characteristic for a first-order transition and in contrast to the prediction of a continuous staging transition. The discontinuity follows from the coexistence of two sets of reflections in the transition region from dominantly stage- $n$  and stage- $(n+1)$  regions. This coexistence may be described as a miscibility gap in the

maximum allowed mixture of stage- $n$  and  $-(n+1)$  packages. The gap size, however, decreases with increasing stage and the staging transition becomes more continuous.

We wish to thank G. Kirczenow, S. A. Safran, S. C. Moss, D. P. DiVencenzo, G. Forgacs, and M. Wortis for valuable discussions, and A. W. Moore of Union Carbide Corporation for donating the highly oriented pyrolytic graphite material. Part of the x-ray measurements were carried out in the Materials Research Laboratory Center for Microanalysis of Materials at the University of Illinois at Urbana-Champaign. This work was supported by the U. S. Department of Energy, Division of Materials Sciences, under Contract No. DE-AC02-76ER01198.

(a) Present address: Department of Physics, University of Houston, University Park, Houston, Tex. 77004.

<sup>1</sup>A stage- $n$  compound refers to a structure in which any two successive intercalate layers are separated by  $n$  carbon planes.

<sup>2</sup>P. Bak and M. H. Jensen, in *Multicritical Phenomena*, edited by R. Pynn and A. Skjeltorp (Plenum, New York, 1984).

<sup>3</sup>S. A. Safran, *Phys. Rev. Lett.* **44**, 937 (1980).

<sup>4</sup>S. E. Millman and G. Kirczenow, *Phys. Rev. B* **26**, 2310 (1982).

<sup>5</sup>G. Kirczenow, *Phys. Rev. Lett.* **52**, 437 (1984), and *Phys. Rev. B* **31**, 5376 (1985).

<sup>6</sup>G. Forgacs and G. Uimin, *Phys. Rev. Lett.* **52**, 6331 (1984).

<sup>7</sup>D. Hohlwein and W. Metz, *Z. Kristallogr.* **139**, 279 (1974).

<sup>8</sup>C. D. Fuerst, T. C. Koch, J. E. Fischer, J. D. Axe, J. B. Hastings, and D. B. McWhan, in *Intercalated Graphite*, edited by M. S. Dresselhaus, G. Dresselhaus, J. E. Fischer, and M. J. Moran, Materials Research Society Symposia Proceedings, Vol. 20 (North-Holland, New York, 1983).

<sup>9</sup>P. A. Heiney, M. E. Huster, V. B. Cajipe, and J. E. Fischer, in Proceedings of the 1984 Materials Research Society Symposium on Graphite Intercalation Compounds: Extended Abstracts, edited by P. C. Eklund, M. S. Dresselhaus, and G. Dresselhaus (unpublished), p. 131.

<sup>10</sup>S. E. Hardcastle, M. E. Misenheimer, and H. Zabel, *Rev. Sci. Instrum.* **54**, 206 (1983).

<sup>11</sup>M. E. Misenheimer and H. Zabel, *Phys. Rev. B* **27**, 1443 (1983).

<sup>12</sup>S. Hendricks and E. Teller, *J. Chem. Phys.* **10**, 147 (1942).

<sup>13</sup>M. E. Misenheimer and H. Zabel, to be published.